Differential roles of ArfGAP1, ArfGAP2, and ArfGAP3 in COPI trafficking

Carolin Weimer, Rainer Beck, Priska Eckert, Ingeborg Reckmann, Jörg Moelleken, Britta Brügger, and Felix Wieland

Heidelberg University Biochemistry Center, D-69120 Heidelberg, Germany

The formation of coat protein complex I (COPI)–coated vesicles is regulated by the small guanosine triphosphatase (GTPase) adenosine diphosphate ribosylation factor 1 (Arf1), which in its GTP-bound form recruits coatomer to the Golgi membrane. Arf GTPase-activating protein (GAP) catalyzed GTP hydrolysis in Arf1 triggers uncoating and is required for uptake of cargo molecules into vesicles. Three mammalian ArfGAPs are involved in COPI vesicle trafficking; however, their individual functions remain obscure. ArfGAP1 binds to membranes depending on their curvature. In this study, we show that ArfGAP2 and ArfGAP3 do not bind directly to membranes but are recruited via interactions with coatomer. In the presence of coatomer, ArfGAP2 and ArfGAP3 activities are comparable with or even higher than ArfGAP1 activity. Although previously speculated, our results now demonstrate a function for coatomer in ArfGAP-catalyzed GTP hydrolysis by Arf1. We suggest that ArfGAP2 and ArfGAP3 are coat protein–dependent ArfGAPs, whereas ArfGAP1 has a more general function.

Introduction

Coat protein complex I (COPI) vesicles are involved in transport processes within the early secretory pathway (Bethune et al., 2006). For their biogenesis, the small GTPase ADP ribosylation factor 1 (Arf1) in its GDP-bound form is recruited to the Golgi membrane by dimeric transmembrane proteins of the p24 family (Gommel et al., 2001) or by interaction with membrin (Honda et al., 2005). The membrane-associated Arf guanine nucleotide exchange factor GBF1 catalyzes exchange of the bound GDP to GTP (Zhao et al., 2006). Arf1-GTP dissociates from the p24 proteins and is inserted into the Golgi membrane (Franco et al., 1996; Antonny et al., 1997) as a dimer (Beck et al., 2008) to recruit the heptameric protein complex coatomer (Palmer et al., 1993). Coatomer polymerization leads to the formation of a COPI-coated vesicle (Bremser et al., 1999; Reinhard et al., 1999). Arf GTPase-activating proteins (GAPs) catalyze hydrolysis of the GTP bound to Arf1 followed by dissociation of the coat (Tanigawa et al., 1993; Cukierman et al., 1995; Reinhard et al., 2003). In addition to this role in uncoating, GTP hydrolysis on Arf1 is essential for efficient uptake of cargo into vesicles (Nickel et al., 1998; Malsam et al., 1999; Pepperkok et al., 2000; Lanoix et al., 2001).

The ArfGAP family of cytosolic proteins is characterized by a well-conserved catalytical zinc finger domain, whereas their noncatalytical domains differ between subgroups of the family (Randazzo and Hirsch, 2004). Two ArfGAPs have been implicated in COPI transport in yeast, Gcs1 and Glo3 (Poon et al., 1999). Both proteins provide overlapping functions and can restore single knockouts of the respective other ArfGAP, but a double knockout of Gcs1 and Glo3 is lethal. The mammalian homologue of Gcs1, ArfGAP1, was the first ArfGAP to be identified (Cukierman et al., 1995; Makler et al., 1995), and its role in COPI trafficking has been studied intensively (Huber et al., 1998; Goldberg, 1999; Bigay et al., 2003; Liu et al., 2005). ArfGAP2 and ArfGAP3, both mammalian homologues of Glo3, have been shown only recently to be involved in COPI vesicle trafficking (Frigerio et al., 2007). Consistent with the findings in yeast, triple knockdowns in mammalian cells are lethal, whereas cells can survive when only ArfGAP1 or both ArfGAP2 and ArfGAP3 are silenced.

ArfGAP1, ArfGAP2, and ArfGAP3 show high sequence similarity within the very N-terminal catalytical domain. In ArfGAP1, two ArfGAP1 lipid packing sensory (ALPS) motifs have been identified within the noncatalytical domain (Bigay et al., 2005; Mesmin et al., 2007). ALPS motifs are unstructured in

Correspondence to F. Wieland: felix.wieland@bzh.uni-heidelberg.de

Abbreviations used in this paper: ALPS, ArfGAP1 lipid packing sensory; Arf, ADP ribosylation factor; COP, coat protein complex; GAP, GTPase-activating protein; NRK, normal rat kidney.

The online version of this article contains supplemental material.

The Rockefeller University Press $30.00
J. Cell Biol. Vol. 183 No. 4 725–735
www.jcb.org/cgi/doi/10.1083/jcb.200806140

solution but form an amphipathic α helix once bound to highly curved membranes as present on a vesicle. Because of this binding behavior, ArfGAP1 displays curvature-dependent ArfGAP activity in vitro, a mechanism suggested to ensure high uncoating efficiency on vesicles, whereas basal activity on flat membranes is rather low (Bigay et al., 2003, 2005). The noncatalytical domains of ArfGAP2 and ArfGAP3 differ from that of ArfGAP1 and show 50% overall sequence identity (Frigerio et al., 2007). There is evidence for an essential functional role of a highly conserved C-terminal motif, the Glo3 motif, which has not been further characterized (Yahara et al., 2006). A recent study revealed that the noncatalytical domains of ArfGAP2 and ArfGAP3 interact with coatomer (Frigerio et al., 2007).

A role of coatomer in ArfGAP-mediated GTP hydrolysis has been studied in different systems. A 100–1,000-fold stimulatory effect of coatomer on GTP hydrolysis was described for the catalytical domain of ArfGAP1 when a soluble version of Arf1, NΔ17Arf1, was used (Goldberg, 1999). However, only very weak (less than twofold) stimulation by coatomer of full-length ArfGAP1 was found in an assay using full-length myristoylated Arf1 on Golgi membranes. In contrast, the activity of Glo3 was increased significantly (∼50-fold) in the presence of coatomer (Szafer et al., 2001).

Previous work on ArfGAP activities in COPI vesicle trafficking does not explain functionally the existence of several ArfGAPs (Huber et al., 1998; Yang et al., 2002; Liu et al., 2005; Frigerio et al., 2007). Therefore, the purpose of this study was to characterize the three mammalian ArfGAPs involved in COPI vesicle trafficking with respect to their individual mechanisms. To this end, the recombinant proteins were expressed in insect cells, purified, and characterized. We find that, in contrast to ArfGAP1, ArfGAP2 and ArfGAP3 activities are dependent on coatomer. From our data, we conclude that coatomer is required for efficient recruitment of ArfGAP2 and ArfGAP3 to the Golgi membrane. Once recruited by coatomer, ArfGAP2 and ArfGAP3 exhibit a strikingly higher activity than ArfGAP1. Two different mechanisms regulate the activities of the three ArfGAPs: binding to membranes by ALPS motifs in the case of ArfGAP1 and recruitment via binding to coatomer in the case of ArfGAP2 and ArfGAP3. These two mechanisms implicate different roles of the three ArfGAPs: ArfGAP2 and ArfGAP3 are the coat protein–dependent ArfGAPs, whereas ArfGAP1 has COPI-dependent as well as COPI-independent functions.

Results

Expression and purification of recombinant ArfGAP1, ArfGAP2, and ArfGAP3 in Sf9 cells

Recombinant ArfGAP1 (Huber et al., 2001) as well as ArfGAP2 and ArfGAP3 (Liu et al., 2001; Singh et al., 2001; Frigerio et al., 2007) have been described previously, however derived from different species and expression systems. To compare biochemically the individual functions of ArfGAP activities, we produced ArfGAP1, ArfGAP2, and ArfGAP3 as recombinant proteins from an equivalent source. *Rattus norvegicus* cDNAs were cloned into the bacterial donor vector pFastBac HTb, which provides the coding sequence for an N-terminal His_6 tag. The tagged versions of the three ArfGAPs are depicted schematically in Fig. 1 A. With the derived recombinant baculovirus stocks, suspension cultures of Sf9 insect cells were infected and incubated for 72 h at 27°C (see Materials and methods). Overexpression of the three fusion proteins was achieved, as shown in Fig. 1 B. The proteins appear as the major bands in the respective cell lysates. The proteins were purified from cell lysates by standard Ni affinity chromatography, resulting in a typical yield of 5–10 mg of highly pure and soluble protein from 500 ml of suspension culture. From lanes E in Fig. 1 B, we deduce that the purity of the proteins was >90%.

Ultrastructural localization of ArfGAPs in mammalian cells

As a basis for the biochemical characterization of the ArfGAPs, the localization of the three enzymes within the early secretory pathway was analyzed by immunogold electron microscopy. To this end, antibodies were raised in rabbits directed against synthetic peptides according to sequences of the rat proteins (see Materials and methods). Ultrathin cryosections of normal rat kidney (NRK) cells were analyzed, as depicted in Fig. 2 A. In correlation to the localization of the cis-Golgi marker GM130, we determined the relative distribution of each ArfGAP to the cis- or trans-half of the Golgi in a way similar to a study of the localization of coatomer isoforms (Moelleken et al., 2007). Statistical evaluation of the data reveals that ArfGAP1 is evenly distributed between the cis- and the trans-half of the Golgi apparatus, whereas both ArfGAP2 and ArfGAP3 display a weak but significant preference for the cis-half of the organelle (Fig. 2 B).

Quantification of ArfGAPs in mammalian cells

The contribution of individual ArfGAP activities in vivo depends not only on the enzymatic activities but also on the relative abundances of the proteins within the cell. To assess the concentration of each ArfGAP, we quantified the proteins in NRK cell lysates by Western blotting. The concentrations of analyte determined in picomoles per milligram of total protein are illustrated in Fig. 2 C. As a result, ArfGAP1 represents the majority of the three ArfGAPs involved in COPI trafficking with ArfGAP3 at a twofold and ArfGAP2 at a 10-fold lower concentration. Thus, the Glo3 homologues, ArfGAP2 and ArfGAP3, together make up about one third of the three ArfGAPs. In a similar way, Arf1 and coatomer concentrations were determined. As expected, Arf1 occurs at the highest molar concentration of the components involved in COPI vesicle formation followed by coatomer and by the ArfGAPs, as shown in Fig. 2 C. For a functional characterization, the purified proteins were analyzed by the in vitro activity assays and binding studies described in the following paragraph.

ArfGAP2 and ArfGAP3 display weak and curvature-independent activity in a liposome-based GAP assay

ArfGAP1 and its yeast homologue Gcs1 were reported to catalyze GTP hydrolysis in Arf1 in a liposome-based fluorimetric

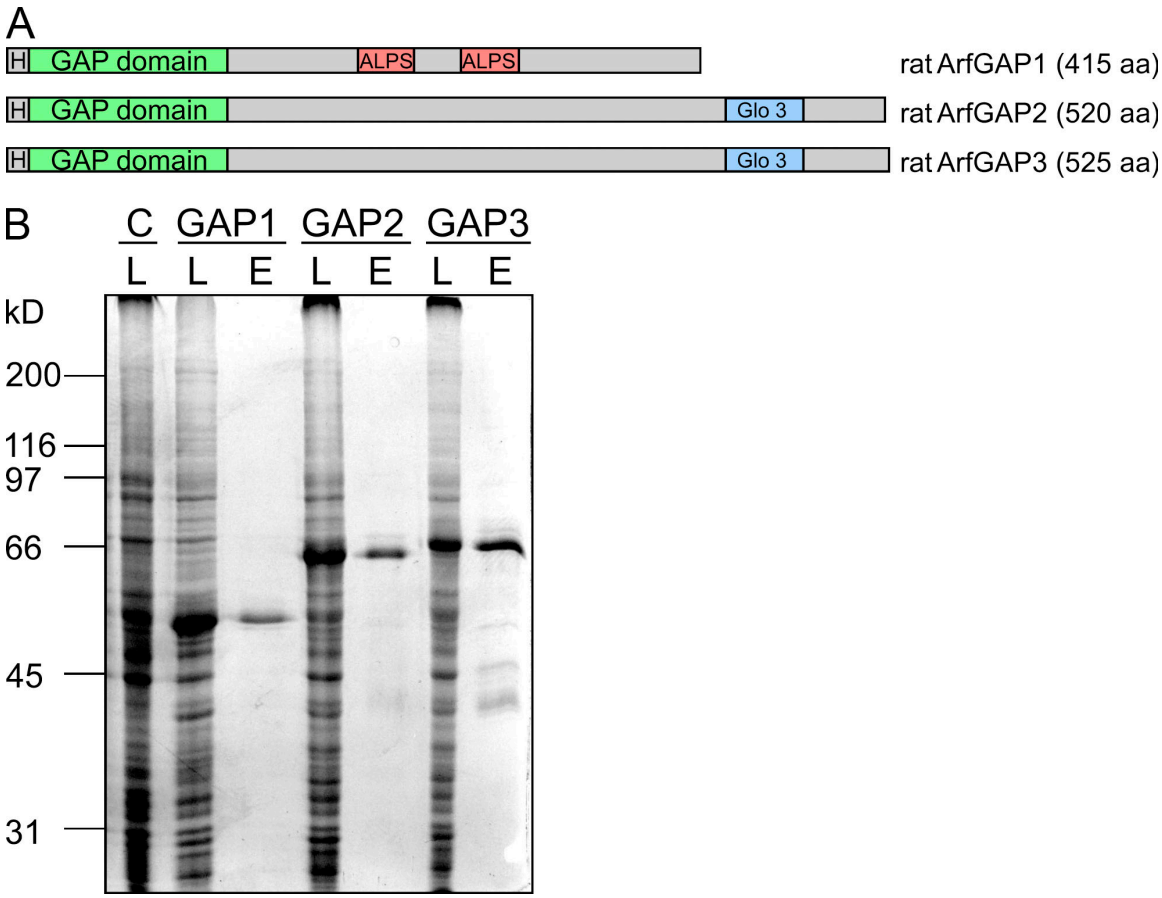

Figure 1. **Expression and purification of recombinant ArfGAP1, ArfGAP2, and ArfGAP3 in Sf9 insect cells.** (A) Schematic view of the recombinant fusion proteins of ArfGAP1, ArfGAP2, and ArfGAP3 used in this study. H, His_6 tag. (B) Expression and purification of the recombinant ArfGAPs. Suspension cultures of Sf9 insect cells were infected with recombinant baculovirus containing the coding sequences for rat ArfGAP1, ArfGAP2, or ArfGAP3 fused to an N-terminal His_6 tag. Cells were harvested after 72 h of incubation, and lysates (L) of cells infected with recombinant baculovirus and of noninfected control cells (C) were analyzed for expression of the recombinant proteins by SDS-PAGE and Coomassie staining. Proteins were purified by Ni affinity chromatography, and 2 µg of the eluates (E) were loaded for SDS-PAGE.

assay (Bigay and Antonny, 2005). GAP activity was observed to be increased on highly curved membranes because of increased binding of the ALPS motif to the liposomes. Therefore, we compared the activities of ArfGAP1 with ArfGAP2 and ArfGAP3 in the same assay. GAP-catalyzed GTP hydrolysis in Arf1 was measured as described by Bigay et al. (2005) on liposomes of 200- or 30-nm diameter in a spectrofluorometer. The exchange of GDP for GTP on myristoylated full-length Arf1 is measured as an increase in tryptophan fluorescence. After the addition of ArfGAPs, fluorescence decreases because of GTP hydrolysis (Fig. 3).

As expected, ArfGAP1 displayed curvature-dependent activity: on liposomes extruded through 200-nm polycarbonate filters, GTP hydrolysis was significantly slower than on liposomes extruded through 30-nm filters (Fig. 3 A). Under the same experimental conditions, we examined ArfGAP2 and ArfGAP3 (Fig. 3, B and C). For both ArfGAP2 and ArfGAP3, we observed a basal activity weaker by a factor of 5–10 compared with ArfGAP1, although all three GAPs share a highly conserved catalytical domain (Frigerio et al., 2007). Additionally, no influence of membrane curvature was observed, indicating the absence of an ALPS-like motif in the noncatalytical domains of ArfGAP2 and ArfGAP3. At high concentrations of ArfGAP proteins, a decrease of fluorescence intensity below the initial level of Arf1-GDP was observed (as depicted for 1 µM ArfGAP2 in Fig. 3 B). This is most likely caused by thermal instability of the ArfGAP protein, as shown in Fig. S1 (available at http://www.jcb.org/cgi/content/full/jcb.200806140/DC1). The weaker activity of ArfGAP2 and ArfGAP3 might either be a characteristic of the Glo3 homologues or could be caused by the assay conditions (i.e., the lipid composition or requirements for certain activation factors).

ArfGAP2 and ArfGAP3 fail to bind to liposomes

To address the question of whether the weaker activities of ArfGAP2 and ArfGAP3 compared with ArfGAP1 correlate with a different binding behavior to liposomes, we performed flotation assays on sucrose density gradients (Bigay and Antonny, 2005). The fractions containing liposomes were analyzed for bound proteins by Western blotting with specific peptide antibodies raised against each of the ArfGAPs.

Curvature-dependent binding of ArfGAP1 to the membranes as shown by Bigay et al. (2005) was reproduced. As shown

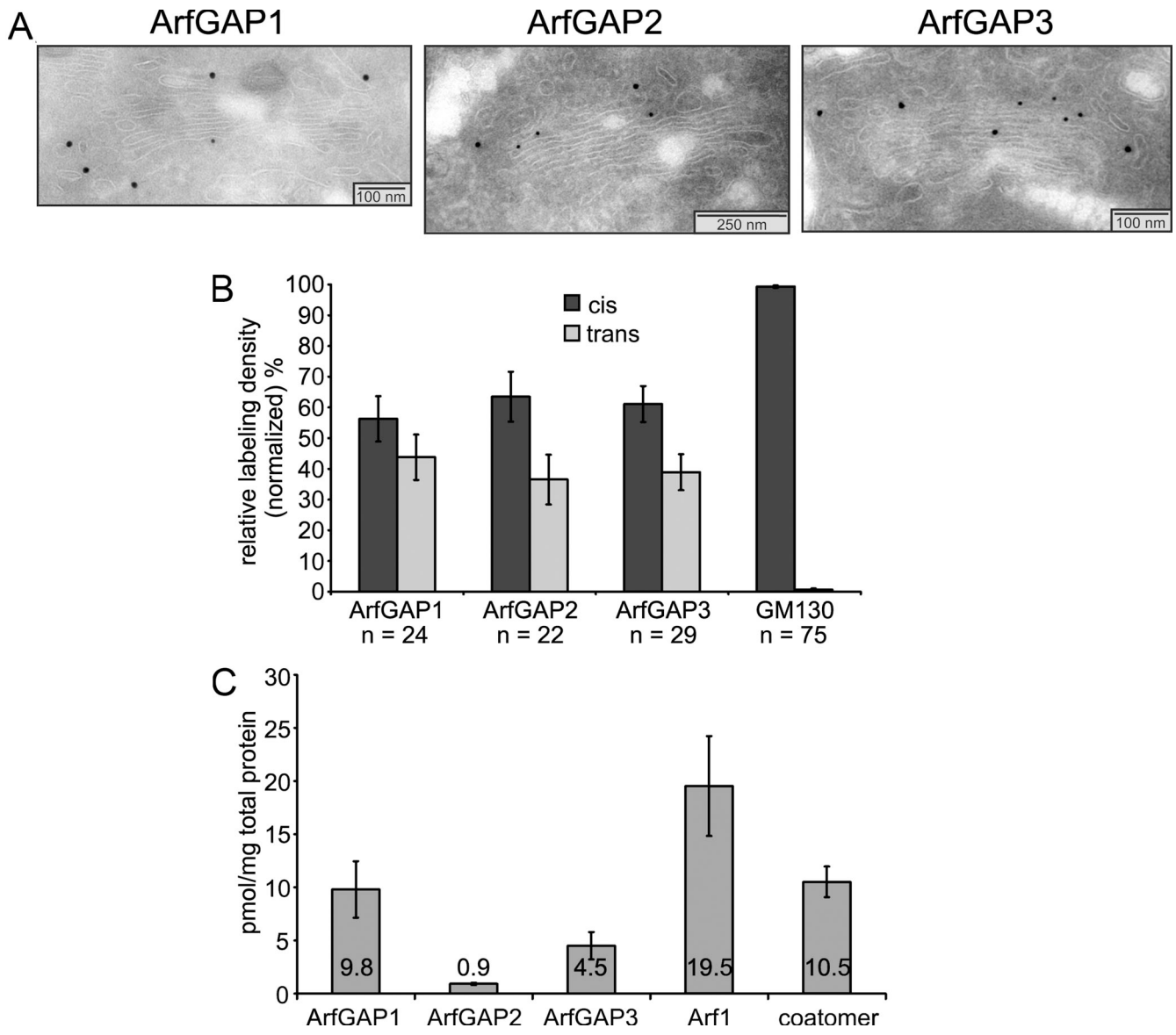

Figure 2. **Quantification and ultrastructural localization of ArfGAPs in mammalian cells.** (A and B) Ultrastructural localization of ArfGAPs. Ultrathin cryosections of NRK cells were stained with antibodies specific for ArfGAP1, ArfGAP2, or ArfGAP3 followed by incubation with protein A–coupled gold particles of 15-nm size. GM130 antibody was used as a cis-Golgi marker and visualized with protein A–coupled gold particles of 10-nm size. (A) Micrographs of representative evaluated Golgis. (B) Statistical evaluation of the normalized relative labeling densities of the three ArfGAPs at cis- and trans-halves of the Golgi. n, number of Golgis evaluated. (C) Quantification of ArfGAPs in mammalian cells. Lysates of NRK cells were separated by SDS-PAGE and stained with antibodies against ArfGAP1, ArfGAP2, ArfGAP3, Arf1, and ε-COP in Western blots. Signals were quantified on the basis of standards of the respective recombinant proteins. The diagram shows the amounts in picomoles per milligram of total protein in the lysates of seven independent experiments. (B and C) Error bars represent standard deviations of the mean.

in Fig. 4 A, ∼10% of the input is bound to the largest liposomes (200 nm), and binding is increased fivefold when the liposomal diameter was reduced to 30 nm, which is consistent with published data. In comparison, ArfGAP2 and ArfGAP3 fail to bind to liposomes under these experimental conditions.

These results explain the differences in GAP activity observed in the fluorimetric measurements (Fig. 3) because under these conditions ArfGAP2 and ArfGAP3 are not concentrated at the liposomal surface where their substrate Arf1-GTP is located. Therefore, higher concentrations of ArfGAP2 and ArfGAP3 are required to reach enzymatic activities similar to ArfGAP1.

ArfGAP1, ArfGAP2, and ArfGAP3 are recruited to the Golgi membrane by different mechanisms

According to immunofluorescence experiments (Cukierman et al., 1995; Frigerio et al., 2007) and immunogold-labeling experiments (Fig. 2 A), all three ArfGAPs are found to be located to Golgi membranes. Therefore, we next addressed the question by which mechanism ArfGAP2 and ArfGAP3 are recruited to the membrane if not by direct binding to the lipid bilayer. A promising candidate to mediate this binding was coatomer, the COP of COPI vesicles, because interaction with coatomer of ArfGAP2 and ArfGAP3 was described previously (Frigerio et al., 2007).

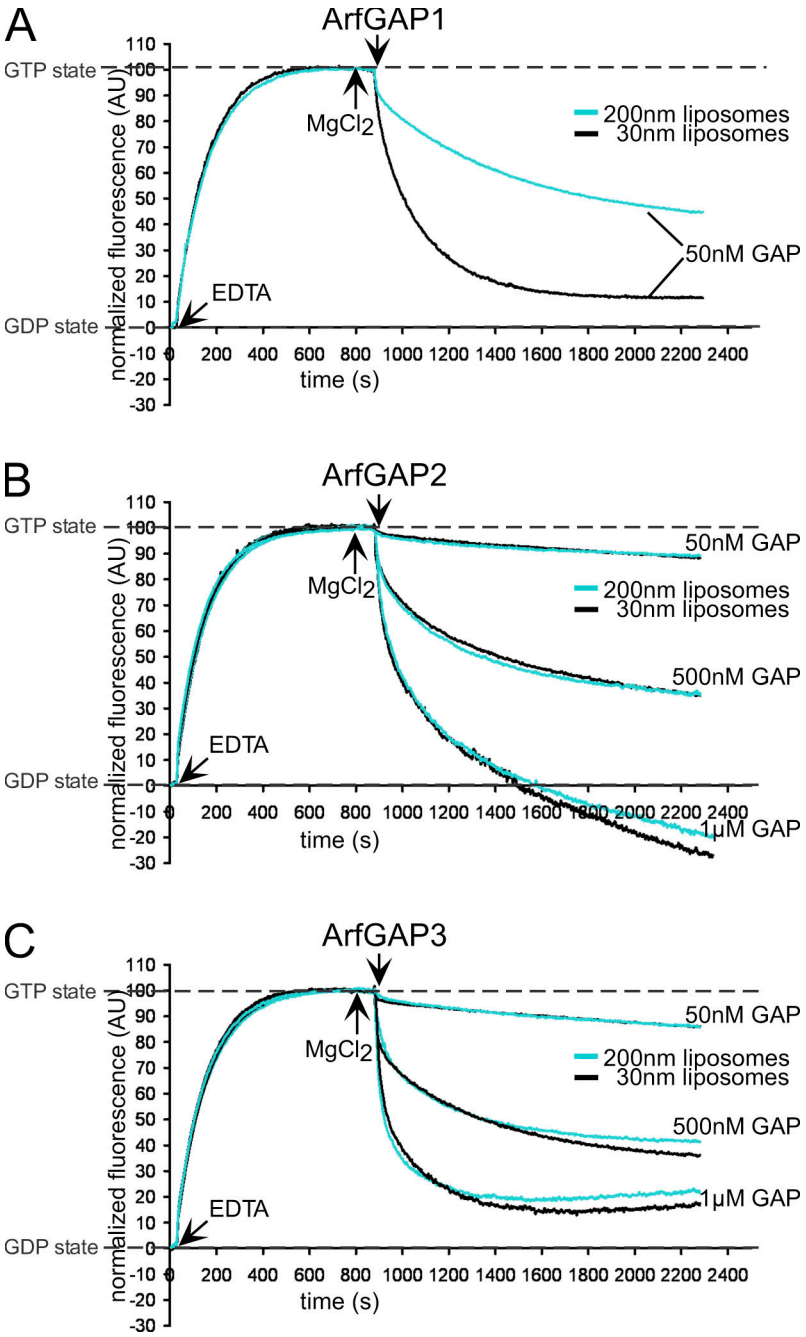

Figure 3. **Activity of ArfGAP1, ArfGAP2, and ArfGAP3 on liposomes of different sizes.** GAP activity was measured by following the change of tryptophan fluorescence in Arf1 (Bigay et al., 2005). Buffer, liposomes extruded through 200- or 30-nm polycarbonate filters, myristoylated full-length Arf1 (1-μM final concentration), and GTP were mixed in a cuvette. After the addition of EDTA, the fluorescence increases because of the exchange of GDP for GTP in Arf1. The GTP state was stabilized by increasing the Mg^{2+} concentration at the indicated time points. ArfGAPs were added to a final concentration of 50 nM, 500 nM, or 1 μM, resulting in a decrease of tryptophan fluorescence caused by GTP hydrolysis. For comparative analysis, fluorescence at time point 0 was set to 0 arbitrary units (AU), fluorescence of the GTP state was normalized to 100 AU, and the shift in fluorescence resulting from tryptophan residues in the ArfGAP proteins was subtracted. For each ArfGAP concentration and liposomal diameter, at least three curves were averaged.

To investigate this possibility, we incubated Golgi membranes with ArfGAPs in the presence or absence of the coat proteins coatomer and Arf1. After centrifugation, the pelleted membranes were analyzed for bound proteins (Fig. 4 B).

We observed binding of 20–30% of the provided ArfGAP1 to Golgi membranes (Fig. 4 B, lane 9). The amount of bound protein is not affected by the presence of Arf1-GTPγS (Fig. 4 B, lane 10), and only a small increase, by less than a factor of two, is found when coatomer was provided additionally (Fig. 4 B, lane 11). In contrast, almost no ArfGAP2 and ArfGAP3 were detected on the Golgi membranes in the presence or absence of Arf1-GTPγS (Fig. 4 B, lanes 9 and 10). However, binding is significantly increased when coatomer is bound to the Golgi (Fig. 4 B, lane 11). These results are consistent with previous findings that ArfGAP2 and ArfGAP3 bind to coatomer, as shown in pull-down assays (Watson et al., 2004; Frigerio et al., 2007).

In summary, these results suggest that the three ArfGAPs are recruited to the Golgi membrane in comparable amounts but by different mechanisms. ArfGAP1 inserts directly into the membrane via its ALPS domains, preferentially at sites with high curvature, whereas ArfGAP2 and ArfGAP3 bind to coatomer and thereby are recruited indirectly to the membrane.

The three ArfGAPs antagonize the formation of coated vesicles in a COPI-budding assay

To test the effect of ArfGAPs on COPI-coated vesicle formation, we performed COPI vesicle–budding assays using Golgi

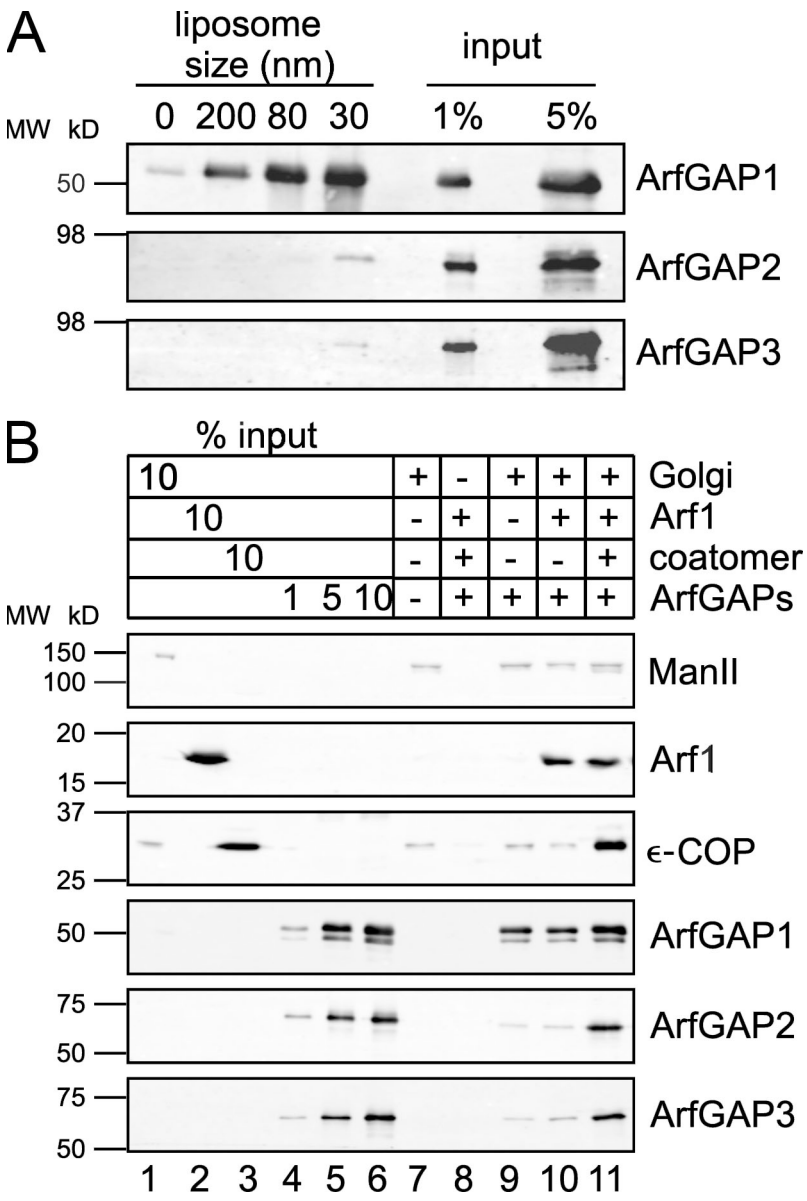

Figure 4. **Binding of ArfGAPs to membranes.** (A) Binding of ArfGAPs to liposomes of different sizes. ArfGAPs were mixed with liposomes (extruded through 200-, 80-, or 30-nm filters, or no liposomes as a control) to a final concentration of 0.5 μM of protein and 0.5 mM of lipids in a total volume of 200 μl. After 5 min of incubation at RT, the samples were floated to an interphase between 25 and 0% (wt/vol) sucrose. 10% of the collected fractions were analyzed for the presence of ArfGAPs by SDS-PAGE and Western blotting with specific antibodies against ArfGAP1, ArfGAP2, and ArfGAP3 and were compared with 1 and 5% of the input. (B) Binding of ArfGAPs to Golgi membranes. Rat liver Golgi membranes were incubated with ArfGAP proteins, myristoylated Arf1, coatomer, and the slowly hydrolyzable GTP analogue GTPγS in the combinations indicated. Golgi membranes were pelleted through a 20% (vol/vol) sucrose cushion, and 30% of the sample was analyzed for bound proteins by SDS-PAGE and Western blotting with antibodies directed against the indicated proteins. MW, molecular weight.

membranes and recombinant proteins under GTP conditions. Each ArfGAP was titrated into the budding reaction, and COPI-coated vesicles were purified by sucrose density centrifugation defined by their buoyant density (see Materials and methods). Fractions were analyzed for vesicle yield as determined by Western blot signals for the transmembrane protein p23 and the coat proteins Arf1 and coatomer. The signals were normalized to an experiment without added ArfGAPs, as depicted in Fig. 5 A.

We found that all three ArfGAPs behave similarly with regard to the yield of COPI-coated vesicles. For a reduction of vesicle yield to 50%, a concentration as low as 1 nM ArfGAP1, ArfGAP2, or ArfGAP3 (corresponding to a 1:1,000 molar ratio of ArfGAP to Arf1) was sufficient. In all three cases, a 10× higher concentration (10 nM) resulted in almost complete loss of vesicle signals, whereas a 10× lower concentration (0.1 nM) was not sufficient to cause significant reduction of vesicle yield (Fig. 5 B).

As the assay was performed with Golgi membranes in the presence of coatomer, all three ArfGAPs should be recruited to the membrane (Fig. 4 B), where they can act on their substrate Arf1-GTP. These results suggest a similar GAP activity of ArfGAP1, ArfGAP2, and ArfGAP3 either caused by direct membrane binding or recruitment by coatomer. However, with this assay it is not possible to tell apart inhibition of COPI-coated vesicle formation (caused by rapid release of Arf1 from the membrane) from rapid uncoating of COPI-coated vesicles.

Collectively, these data show that the three ArfGAPs antagonize the yield of COPI-coated vesicles to roughly the same extent. To more precisely quantify uncoating activities, static light–scattering assays with COPI-coated liposomes as well as Golgi membranes were performed.

ArfGAP2 and ArfGAP3 are more efficient in uncoating than ArfGAP1

ArfGAP-catalyzed GTP hydrolysis in Arf1 leads to uncoating of COPI vesicles (Tanigawa et al., 1993; Cukierman et al., 1995; Reinhard et al., 2003). To assess the activities of the three

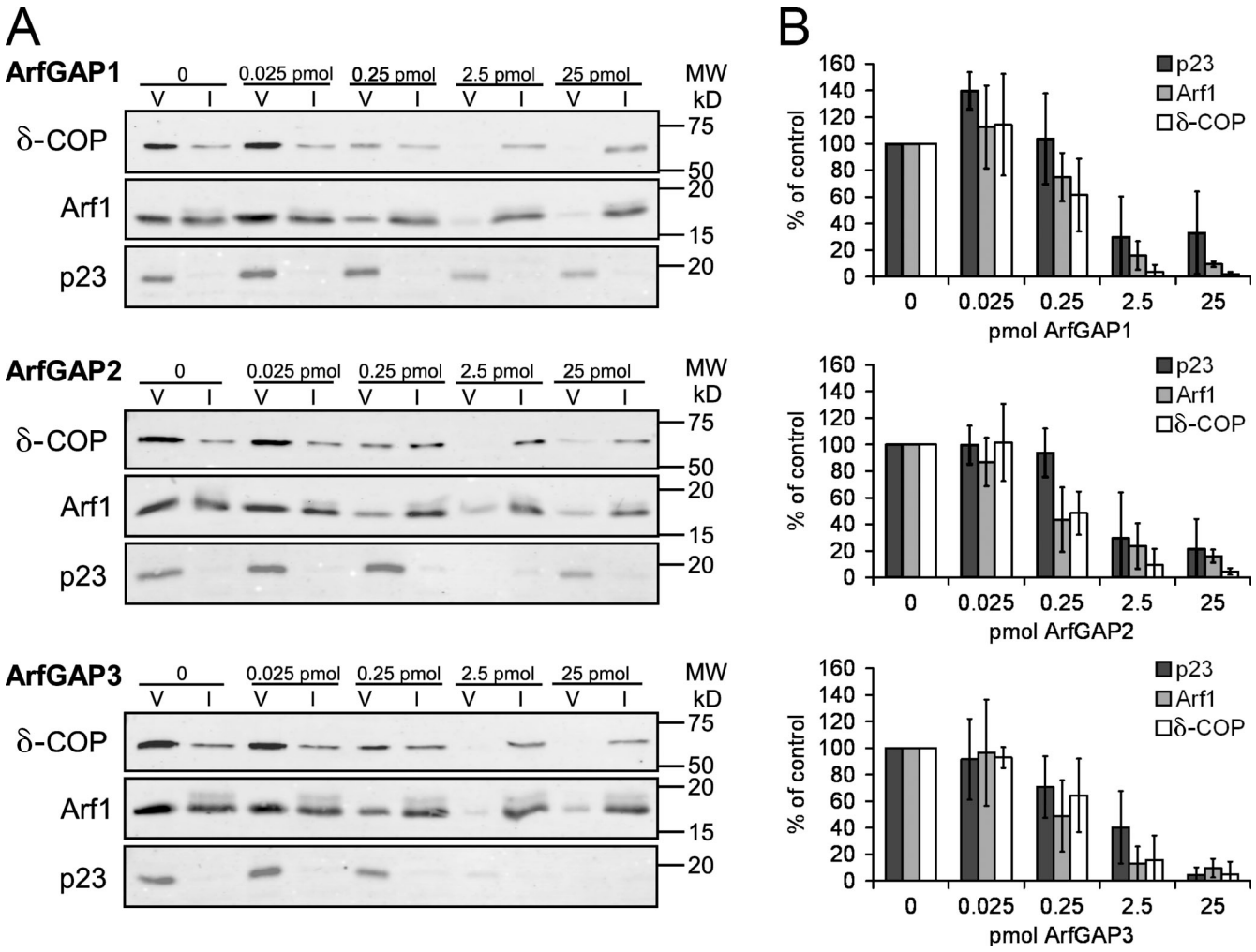

Figure 5. **Quantification of uncoating activities of ArfGAPs in COPI vesicle formation.** (A) COPI vesicles were formed using salt-washed Golgi membranes and recombinant proteins in the presence of varying amounts of ArfGAP1, ArfGAP2, or ArfGAP3. COPI-coated vesicles were purified via sucrose density centrifugation. 50% of the vesicle fractions (V) and 0.5% of input (I) were analyzed by Western blotting with antibodies directed against δ-COP, Arf1, and p23. MW, molecular weight. (B) Western blot signals for p23, Arf1, and δ-COP were quantified and normalized to the signals in control reactions without the addition of ArfGAP. Results of three independent experiments were averaged. Error bars represent standard deviations of the mean.

ArfGAPs in this process, we used a light-scattering assay as described previously (Bigay and Antonny, 2005) that allows observance of the assembly–disassembly cycle of the COPI coat. To this end, liposomes containing p23 lipopeptide (Nickel and Wieland, 2001) are incubated with Arf1, coatomer, and EDTA. The coating reaction is started by the addition of GTP and is followed by a proportional increase in light scattering. After reaching a plateau, the GTP state of Arf1 was stabilized by the addition of Mg^{2+}, and uncoating of the liposomes was initiated by the addition of the individual ArfGAPs.

To control for the requirement of GTP hydrolysis in the uncoating reaction, liposomes were analyzed that were coated in the presence of the poorly hydrolyzable GTP analogue GTPγS. As shown in Fig. 6 B, uncoating after the addition of ArfGAPs was prevented, linking the uncoating reaction to the activity of the ArfGAPs.

As depicted in Fig. 6, a marked decrease in light scattering was observed after the addition of ArfGAPs in the presence of GTP. In Fig. 6 (A–C), liposomes extruded through 200-, 80-, or 30-nm pores (mean diameters of 160 nm, 60 nm, and 40 nm, respectively, as assessed by dynamic light scattering; Fig. S2, available at http://www.jcb.org/cgi/content/full/jcb.200806140/DC1) were used to assess uncoating activities in the dependence of membrane curvature. Whereas a strong increase in uncoating activity of ArfGAP1 was observed between 160- and 60-nm liposomes, a decrease in diameter to 40 nm did not further enhance the activity. This was not surprising given the similar size of the liposomes as assessed by dynamic light scattering.

To investigate the ArfGAP activities under more physiological conditions, static light–scattering experiments were performed with Golgi-enriched membranes. As depicted in Fig. 6 D, on Golgi membranes the three ArfGAPs qualitatively showed activities similar to those on liposomes.

Quantification of initial reaction rates showed ratios of ArfGAP1 to ArfGAP2/ArfGAP3 activities of ∼1:10 for 160-nm liposomes, ∼1:5 for 60- or 40-nm liposomes, and 1:3 for Golgi membranes. This may either reflect the presence of additional ArfGAP effectors on the Golgi or preferential coating at

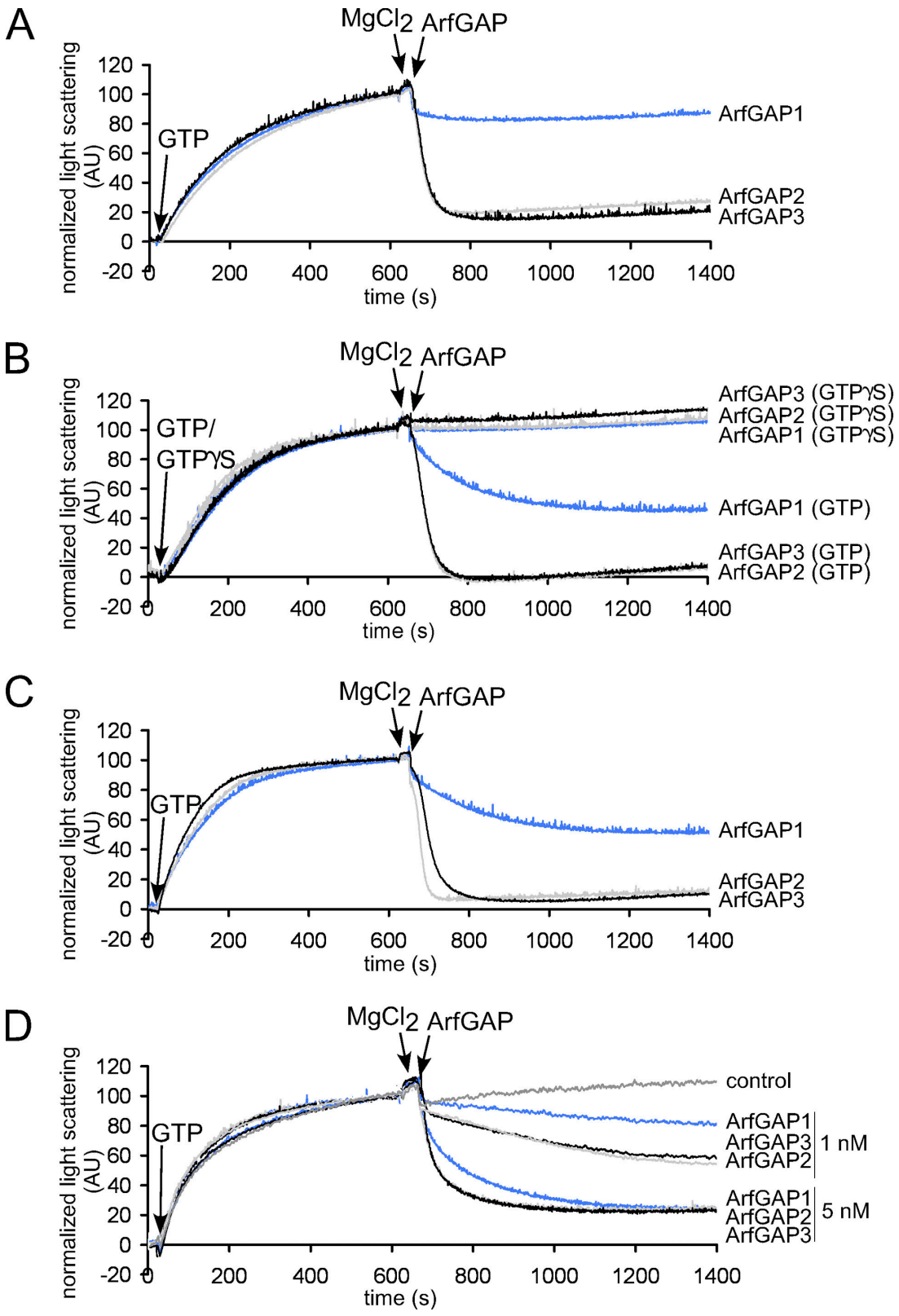

Figure 6. **Uncoating activities of ArfGAPs measured by light scattering.** (A–D) The coat assembly–disassembly cycle was measured by light scattering at 350 nm in a spectrofluorometer. Liposomes supplemented with 2 mol% of p23 lipopeptide and extruded through 200-, 80-, or 30-nm polycarbonate filters (dynamic light-scattering assays showed a mean diameter of 160 nm, 60 nm, and 40 nm, respectively; Fig. S2, available at http://www.jcb.org/cgi/content/full/jcb.200806140/DC1) or salt-washed Golgi membranes were incubated with Arf1, coatomer, and EDTA. At the time points indicated, GTP or its slowly hydrolyzable analogue GTPγS was added to start the coating reaction. After 10 min, the GTP state was stabilized with $MgCl_2$. ArfGAPs (ArfGAP1, blue lines; ArfGAP2, gray lines; ArfGAP3, black lines) were added at the indicated time points to induce coat disassembly. Scattering at time point 0 was set to 0 AU, and scattering of the coated state was normalized to 100 AU. (A) 160 nm liposomes and 2.5 nM ArfGAPs; (B) 60 nm liposomes and 2.5 nM ArfGAPs; (C) 40 nm liposomes and 2.5 nM ArfGAPs; (D) Golgi membranes and 1 and 5 nM ArfGAPs.

sites with high curvature. In summary, when analyzed in the COPI-budding assay, the three ArfGAPs showed comparable activities, whereas in the uncoating assay, the activities of ArfGAP2 and ArfGAP3 are markedly higher.

Discussion

Although a role of ArfGAP1 in COPI vesicle trafficking has been described in some detail in the past (Cukierman et al., 1995; Makler et al., 1995; Huber et al., 1998; Goldberg, 1999; Bigay et al., 2003; Liu et al., 2005), an involvement of the two human homologues of Glo3, ArfGAP2 and ArfGAP3, in COPI-mediated transport was reported only recently (Frigerio et al., 2007). Studies in yeast point to an important role of Glo3 in retrograde transport (Dogic et al., 1999; Poon et al., 1999; Lewis et al., 2004). To elucidate functions of the three mammalian ArfGAPs in COPI trafficking, we analyzed their ultrastructural localizations and biochemical properties. We find that ArfGAP2 and ArfGAP3 localized across the Golgi stacks in a weak but significant gradient from the cis to the trans side. ArfGAP1 is distributed quite evenly within the Golgi apparatus, which is in good accordance with a wider range of effectors such as complexes with golgins (Drin et al., 2008). Such a broader range of functions is also consistent with the higher concentration of this enzyme when compared with ArfGAP2 and ArfGAP3. We show that in contrast to ArfGAP1, ArfGAP2 and ArfGAP3 recruitment to the membrane is dependent on coatomer. In the presence of coatomer, ArfGAP2 and ArfGAP3 display even higher activities in uncoating in a liposomal system as well as on Golgi membranes compared with ArfGAP1. In vesicle formation assays, all three ArfGAPs show inhibition at very low catalytic concentrations.

Collectively, we find that regulation of ArfGAP2 and ArfGAP3 activities is based on a mechanism distinct from ArfGAP1, and our results suggest that the roles of the Glo3 homologues in COPI trafficking differ from those of ArfGAP1.

A role of coatomer in ArfGAP-mediated GTP hydrolysis

An effect of coatomer on GTP hydrolysis catalyzed by ArfGAPs has been investigated before, yet its precise role is not clear. Goldberg (1999) analyzed a truncated soluble form of Arf1, NΔ17Arf1, with the catalytical domain of ArfGAP1 in the absence of membranes. In this assay, ArfGAP1 catalytical domain is present at very high concentrations almost stoichiometric to Arf1, suggesting a very low activity of ArfGAP1 in solution. Addition of coatomer to this system results in a strong (up to 1,000-fold) stimulation of GTP hydrolysis, indicating that in solution, Arf1-GTP, when bound to coatomer, represents a better substrate for the ArfGAP. In contrast, Szafer et al. (2000) investigated ArfGAP1 activity in a liposomal system with the full-length protein and myristoylated full-length Arf1. In this assay, GTP hydrolysis activity is observed at a much lower concentration of ArfGAP, in the nanomolar range. This high activity is not further stimulated by the addition of coatomer. This is consistent with an ALPS-dependent binding to membranes of ArfGAP1 (Bigay et al., 2003, 2005) that is not expected to be further enhanced by coatomer. Likewise, on Golgi membranes, only a very weak stimulation of ArfGAP1 activity by coatomer was observed. In contrast, Glo3 activity is highly stimulated by coatomer on Golgi membranes but only weakly on liposomes (Szafer et al., 2001). In light of the data presented in this study, this lack of stimulation on liposomes could be explained by the absence of p24 tails that are required for efficient recruitment of coatomer (Bremser et al., 1999) and thereby of Glo3 to the membrane.

A direct interaction of the yeast Glo3 but not Gcs1 with the coatomer complex has been published (Eugster et al., 2000; Lewis et al., 2004). Moreover, the noncatalytical domains of both Glo3 and ArfGAP2 were found to bind coatomer in almost stoichiometric amounts, as shown by pull-down assays (Frigerio et al., 2007). Collectively, our data explain the role of coatomer in ArfGAP-catalyzed GTP hydrolysis. It seems that coatomer does not provide a catalytical cofactor activity but simply acts as a binding partner of Glo3 homologues for efficient recruitment to the membrane. ArfGAP1 acts independently of coatomer, as it binds to the lipid bilayer by its ALPS domains.

Roles of ArfGAPs in COPI trafficking

The three ArfGAPs are likely to have overlapping functions and are probably able to substitute for each other, as can be deduced from knockdown experiments in yeast and human cells (Poon et al., 1999; Frigerio et al., 2007). However, the two differential modes of membrane binding, coatomer independent in the case of ArfGAP1 and coatomer dependent in the case of ArfGAP2 and ArfGAP3, implicate different roles of the three enzymes. From our data, we conclude that ArfGAP2 and ArfGAP3 are coat protein–dependent ArfGAPs, whereas ArfGAP1 plays a more general role, as its activity does not depend on coatomer. ArfGAP1 has been shown to be involved in COPI-dependent as well as COPI-independent events, such as a regulation of an asymmetrical mode of tethering between flat and curved membranes of the golgin GMAP-210 (Drin et al., 2008), further supporting differential functions of the three ArfGAPs. The strictly coatomer-dependent activities of ArfGAP2 and ArfGAP3 are reminiscent of the mechanism of coat-controlled specificity of GTP hydrolysis that is also found for the COPII and clathrin coats. The Sar1 GAP activity is mediated by a subunit of the COPII coat itself, Sec23 (Yoshihisa et al., 1993; Bi et al., 2002). In clathrin-dependent trafficking, direct specific interactions of the ArfGAPs AGAP1 and AGAP2 with the adapter protein complexes AP-1 and AP-3, respectively, have been shown, ensuring site-specific regulation (Nie et al., 2003, 2005). Whether ArfGAP2 or ArfGAP3 is bound to coatomer already in the cytosol and recruited en bloc with the complex or whether coatomer is bound first and recruits the ArfGAPs in a second step cannot be distinguished at this time. However, the light-scattering data show that ArfGAP2 and ArfGAP3 can be recruited after coatomer has attached to the membrane, and their specific activities in this uncoating assay are markedly higher than that of ArfGAP1. Individual roles of ArfGAP2 and ArfGAP3 will be the subject of future work. One could imagine that the two proteins interact differentially with coatomer isoforms (Futatsumori et al., 2000; Wegmann et al., 2004; Moelleken et al., 2007) and therefore might discriminate between different subpopulations of COPI vesicles comparable with AGAP1 and AGAP2 that distinguish

between the adapter protein complexes AP-1 and AP-3 (Nie et al., 2005). Thus, once coatomer isoforms are available, questions as to the functional differences of ArfGAP2 and ArfGAP3 can be addressed directly.

Materials and methods

Expression and purification of recombinant ArfGAPs
Rat cDNAs (Open Biosystems) coding for ArfGAP1, ArfGAP2, and ArfGAP3 were amplified via PCR and cloned into the pFastBac HTb vector (Invitrogen) via BamHI and XhoI restriction sites. Following the manufacturer's protocol, recombinant virus stocks were gained. For expression, suspension cultures of Sf9 insect cells were infected with viral stocks and incubated at 27°C for 72 h. Cells were lysed in binding buffer (25 mM Hepes-KOH, 300 mM KCl, 5 mM imidazole, and 1 mM DTT, pH 7.4). Proteins were purified from a 100,000 *g* supernatant via Ni affinity chromatography followed by a buffer exchange to 25 mM Hepes-KOH and 150 mM KCl, pH 7.4.

Generation of ArfGAP-specific antibodies
Peptide antibodies specific for ArfGAP1 (GAP1 rab2), ArfGAP2 (GAP2 rab2), and ArfGAP3 (GAP3 rab2) were raised in rabbits (Pineda Antikörper Service) using the following peptides: EPPKAKSPSSDSWTC (ArfGAP1), CTFASGPPKYKDNPFS (ArfGAP2), and CKYQEDPEDSYFSSSSK (ArfGAP3). Antisera were affinity purified and tested for specificity in Western blotting, immunoprecipitation, and immunofluorescence.

Preparation of Arf1, coatomer, and Golgi membranes
Full-length myristoylated human Arf1 was recombinantly expressed and purified as described previously (Franco et al., 1995). Rabbit liver coatomer was purified as described previously (Pavel et al., 1998). Golgi membranes were enriched from rat liver as described previously (Tabas and Kornfeld, 1979).

Liposome preparation
Liposomes of a Golgi-like lipid composition ± p23 lipopeptide (Nickel and Wieland, 2001) were generated as described previously (Bigay et al., 2005) and extruded through polycarbonate filters of 200-, 80-, or 30-nm pore size (Avestin or GE Healthcare). To determine the actual diameter, aliquots of the liposomes were diluted to a final concentration of 0.1 mM in 50 µl of HKM buffer (25 mM Hepes-KOH, 150 mM KCl, and 1 mM $MgCl_2$, pH 7.4) and measured at RT in a Zetasizer instrument (1000HS; Malvern). Data were acquired using the Zetasizer advanced software (1000HS). The measured mean diameters were approximately 160 nm, 60 nm, and 40 nm.

Tryptophan fluorescence assay
ArfGAP activity on liposomes was measured as described previously (Bigay et al., 2005) in a spectrofluorometer (FP-6500; Jasco) at 37°C in HKM buffer in a total volume of 600 µl using 100 µM of liposomes and 1 µM Arf1. GTP exchange was started by the addition of 100 µM GTP and 2 mM EDTA. After 750 s, $MgCl_2$ was added to a final concentration of 4 mM followed by the addition of ArfGAPs to a final concentration of 50 nM, 500 nM, or 1 µM. Fluorescence was normalized to zero before the addition of EDTA (GDP state) and to 100 AU after the addition of $MgCl_2$ (GTP state). The shift in fluorescence caused by the addition of ArfGAPs was subtracted.

As controls, ArfGAP proteins alone (final concentrations of 50 nM, 500 nM, or 1 µM) were added to HKM buffer. Tryptophan fluorescence was measured using the aforementioned parameters. Fluorescence levels at the time points of ArfGAP addition were normalized to 100 AU.

Membrane-binding assays
Flotation experiments with liposomes were performed in HKM buffer as described previously (Bigay and Antonny, 2005) with the following variations. Instead of NBD-labeled lipid, rhodamine-labeled phosphatidylethanolamine (Avanti Polar Lipids, Inc.) was used. After SDS-PAGE, bound proteins were stained by Western blotting with ArfGAP-specific antibodies.

Golgi-binding assays were performed in assay buffer (25 mM Hepes-KOH, 20 mM KCl, and 2.5 mM MgAc, pH 7.2) using the following components: 100 µg of Golgi membranes, 5 µg Arf1, 32 µg coatomer, 0.1 mM GTPγS, and 1 µg of each ArfGAP in a total volume of 200 µl. After incubation for 5 min at RT, the samples were layered on a 300-µl cushion of 20% (vol/vol) sucrose. Golgi membranes were pelleted by centrifugation at 15,000 *g* for 20 min at 4°C in a rotor (SW55Ti; Beckman Coulter), resuspended in sample buffer, and analyzed for bound proteins by SDS-PAGE and Western blotting.

Vesicle-budding assay
To reconstitute COPI vesicles, 0.8 mg of salt-washed Golgi membranes was mixed with 5 µg Arf1, 30 µg coatomer, and 1.2 mM GTP in a total volume of 250 µl. ArfGAPs were titrated in from 0.025–25 pmol. After 10-min incubation at 37°C, the salt concentration was raised to 250 mM KCl. After centrifugation at 12,000 *g* for 5 min, the supernatant containing COPI vesicles was loaded on top of two sucrose cushions (10 µl of 50% sucrose and 50 µl of 37% sucrose) and centrifuged at 100,000 *g* for 50 min in an SW55Ti rotor. COPI-coated vesicles were concentrated at the interphase between 50 and 37% sucrose. 0.5% of the input sample and 50% of the isolated vesicle fraction were analyzed by Western blotting using an Alexa Fluor 680–conjugated goat anti–rabbit secondary antibody (Invitrogen). Signals were quantified using an infrared imaging system and software (Odyssey; LI-COR Biosciences).

Light-scattering assay
Light-scattering assays were performed as described previously (Bigay and Antonny, 2005) using 70 µg/ml of salt-washed Golgi membranes or 0.1 mM Golgi-like liposomes supplemented with 2 mol% p23 lipopeptide, 1 µM Arf1, 2 mM EDTA, and 100 µM GTP or GTPγS in static light–scattering buffer (50 mM Hepes-KOH, pH 7.2, 1 mM $MgCl_2$, 1 mM DTT, and 120 mM KAc) in a total volume of 600 µl. After 10-min incubation at 37°C, 4 mM $MgCl_2$ was added followed by the addition of recombinant ArfGAPs to a final concentration of 1, 2.5, or 5 nM. Scattering was normalized to 0 AU before the addition of GTP and to 100 AU before the addition of $MgCl_2$.

Quantification
NRK cells grown to 80% confluency were trypsinized and suspended in PBS. Cells were pelleted (1 min at 1,000 *g*), washed once with PBS and once with breaking buffer (10 mM Tris-HCl, pH 8, 150 mM NaCl, 0.8 µg/ml pepstatin A, 1 mM *o*-phenanthrolin, and protease inhibitor cocktail [Roche]), resuspended in breaking buffer, and lysed by several passages through 24- and 27-G needles until >90% were broken. Supernatants of a 1,000 *g* centrifugation were analyzed by Western blotting. Known amounts of purified proteins were loaded as standards. Western blot signals were quantified using the Odyssey infrared imaging system.

Immunogold labeling
Immunogold-labeling experiments were performed as described previously (Moelleken et al., 2007). In brief, cryosections of chemically fixed NRK cells were labeled with an ArfGAP-specific antibody followed by incubation with protein A–coupled gold particles of 15-nm size (provided by G. Posthuma, Utrecht University, Netherlands). GM130 antibody (Abcam) was used as a cis-Golgi marker and visualized with 10-nm gold particles conjugated to either protein A or goat anti–mouse antibody (British BioCell International). The sections were contrasted with uranyl acetate and analyzed by transmission electron microscopy (EM 10 CR; Carl Zeiss, Inc.). Digital images were acquired with a 300-s exposure time using a wide angle dual speed SlowScan charge-coupled device camera (WIA-7888-V; Tröndle Restlichtverstärkersysteme) for transmission electron microscopy and the corresponding ImageSP software (Tröndle Restlichtverstärkersysteme). Gold dots of 15 nm representing ArfGAPs were counted, and the relative labeling density at cis- and trans-Golgi was calculated.

Online supplemental material
Fig. S1 shows the kinetics of tryptophan fluorescence of ArfGAP1, ArfGAP2, and ArfGAP3 as a control for the ArfGAP activity assays. Fig. S2 shows the actual diameter of liposomes as measured by dynamic light scattering. Online supplemental material is available at http://www.jcb.org/cgi/content/full/jcb.200806140/DC1.

This work was supported by grants from the Deutsche Forschungsgemeinschaft (SFB638 and GK1188).

Submitted: 23 June 2008
Accepted: 21 October 2008

References

Antonny, B., S. Beraud-Dufour, P. Chardin, and M. Chabre. 1997. N-terminal hydrophobic residues of the G-protein ADP-ribosylation factor-1 insert into membrane phospholipids upon GDP to GTP exchange. *Biochemistry*. 36:4675–4684.

Beck, R., Z. Sun, F. Adolf, C. Rutz, J. Bassler, K. Wild, I. Sinning, E. Hurt, B. Brugger, J. Bethune, and F. Wieland. 2008. Membrane curvature induced by Arf1-GTP is essential for vesicle formation. *Proc. Natl. Acad. Sci. USA.* 105:11731–11736.

Bethune, J., F. Wieland, and J. Moelleken. 2006. COPI-mediated Transport. *J. Membr. Biol.* 211:65–79.

Bi, X., R.A. Corpina, and J. Goldberg. 2002. Structure of the Sec23/24-Sar1 prebudding complex of the COPII vesicle coat. *Nature.* 419:271–277.

Bigay, J., and B. Antonny. 2005. Real-time assays for the assembly-disassembly cycle of COP coats on liposomes of defined size. *Methods Enzymol.* 404:95–107.

Bigay, J., P. Gounon, S. Robineau, and B. Antonny. 2003. Lipid packing sensed by ArfGAP1 couples COPI coat disassembly to membrane bilayer curvature. *Nature.* 426:563–566.

Bigay, J., J.F. Casella, G. Drin, B. Mesmin, and B. Antonny. 2005. ArfGAP1 responds to membrane curvature through the folding of a lipid packing sensor motif. *EMBO J.* 24:2244–2253.

Bremser, M., W. Nickel, M. Schweikert, M. Ravazzola, M. Amherdt, C.A. Hughes, T.H. Sollner, J.E. Rothman, and F.T. Wieland. 1999. Coupling of coat assembly and vesicle budding to packaging of putative cargo receptors. *Cell.* 96:495–506.

Cukierman, E., I. Huber, M. Rotman, and D. Cassel. 1995. The ARF1 GTPase-activating protein: zinc finger motif and Golgi complex localization. *Science.* 270:1999–2002.

Dogic, D., B. de Chassey, E. Pick, D. Cassel, Y. Lefkir, S. Hennecke, P. Cosson, and F. Letourneur. 1999. The ADP-ribosylation factor GTPase-activating protein Glo3p is involved in ER retrieval. *Eur. J. Cell Biol.* 78:305–310.

Drin, G., V. Morello, J.F. Casella, P. Gounon, and B. Antonny. 2008. Asymmetric tethering of flat and curved lipid membranes by a golgin. *Science.* 320:670–673.

Eugster, A., G. Frigerio, M. Dale, and R. Duden. 2000. COP I domains required for coatomer integrity, and novel interactions with ARF and ARF-GAP. *EMBO J.* 19:3905–3917.

Franco, M., P. Chardin, M. Chabre, and S. Paris. 1995. Myristoylation of ADP-ribosylation factor 1 facilitates nucleotide exchange at physiological Mg2+ levels. *J. Biol. Chem.* 270:1337–1341.

Franco, M., P. Chardin, M. Chabre, and S. Paris. 1996. Myristoylation-facilitated binding of the G protein ARF1GDP to membrane phospholipids is required for its activation by a soluble nucleotide exchange factor. *J. Biol. Chem.* 271:1573–1578.

Frigerio, G., N. Grimsey, M. Dale, I. Majoul, and R. Duden. 2007. Two human ARFGAPs associated with COP-I-coated vesicles. *Traffic.* 8:1644–1655.

Futatsumori, M., K. Kasai, H. Takatsu, H.W. Shin, and K. Nakayama. 2000. Identification and characterization of novel isoforms of COP I subunits. *J. Biochem.* 128:793–801.

Goldberg, J. 1999. Structural and functional analysis of the ARF1-ARFGAP complex reveals a role for coatomer in GTP hydrolysis. *Cell.* 96:893–902.

Gommel, D.U., A.R. Memon, A. Heiss, F. Lottspeich, J. Pfannstiel, J. Lechner, C. Reinhard, J.B. Helms, W. Nickel, and F.T. Wieland. 2001. Recruitment to Golgi membranes of ADP-ribosylation factor 1 is mediated by the cytoplasmic domain of p23. *EMBO J.* 20:6751–6760.

Honda, A., O.S. Al-Awar, J.C. Hay, and J.G. Donaldson. 2005. Targeting of Arf-1 to the early Golgi by membrin, an ER-Golgi SNARE. *J. Cell Biol.* 168:1039–1051.

Huber, I., E. Cukierman, M. Rotman, T. Aoe, V.W. Hsu, and D. Cassel. 1998. Requirement for both the amino-terminal catalytic domain and a noncatalytic domain for in vivo activity of ADP-ribosylation factor GTPase-activating protein. *J. Biol. Chem.* 273:24786–24791.

Huber, I., M. Rotman, E. Pick, V. Makler, L. Rothem, E. Cukierman, and D. Cassel. 2001. Expression, purification, and properties of ADP-ribosylation factor (ARF) GTPase activating protein-1. *Methods Enzymol.* 329:307–316.

Lanoix, J., J. Ouwendijk, A. Stark, E. Szafer, D. Cassel, K. Dejgaard, M. Weiss, and T. Nilsson. 2001. Sorting of Golgi resident proteins into different subpopulations of COPI vesicles: a role for ArfGAP1. *J. Cell Biol.* 155:1199–1212.

Lewis, S.M., P.P. Poon, R.A. Singer, G.C. Johnston, and A. Spang. 2004. The ArfGAP Glo3 is required for the generation of COPI vesicles. *Mol. Biol. Cell.* 15:4064–4072.

Liu, W., R. Duden, R.D. Phair, and J. Lippincott-Schwartz. 2005. ArfGAP1 dynamics and its role in COPI coat assembly on Golgi membranes of living cells. *J. Cell Biol.* 168:1053–1063.

Liu, X., C. Zhang, G. Xing, Q. Chen, and F. He. 2001. Functional characterization of novel human ARFGAP3. *FEBS Lett.* 490:79–83.

Makler, V., E. Cukierman, M. Rotman, A. Admon, and D. Cassel. 1995. ADP-ribosylation factor-directed GTPase-activating protein. Purification and partial characterization. *J. Biol. Chem.* 270:5232–5237.

Malsam, J., D. Gommel, F.T. Wieland, and W. Nickel. 1999. A role for ADP ribosylation factor in the control of cargo uptake during COPI-coated vesicle biogenesis. *FEBS Lett.* 462:267–272.

Mesmin, B., G. Drin, S. Levi, M. Rawet, D. Cassel, J. Bigay, and B. Antonny. 2007. Two lipid-packing sensor motifs contribute to the sensitivity of ArfGAP1 to membrane curvature. *Biochemistry.* 46:1779–1790.

Moelleken, J., J. Malsam, M.J. Betts, A. Movafeghi, I. Reckmann, I. Meissner, A. Hellwig, R.B. Russell, T. Sollner, B. Brugger, and F.T. Wieland. 2007. Differential localization of coatomer complex isoforms within the Golgi apparatus. *Proc. Natl. Acad. Sci. USA.* 104:4425–4430.

Nickel, W., and F.T. Wieland. 2001. Receptor-dependent formation of COPI-coated vesicles from chemically defined donor liposomes. *Methods Enzymol.* 329:388–404.

Nickel, W., J. Malsam, K. Gorgas, M. Ravazzola, N. Jenne, J.B. Helms, and F.T. Wieland. 1998. Uptake by COPI-coated vesicles of both anterograde and retrograde cargo is inhibited by GTPgammaS in vitro. *J. Cell Sci.* 111:3081–3090.

Nie, Z., M. Boehm, E.S. Boja, W.C. Vass, J.S. Bonifacino, H.M. Fales, and P.A. Randazzo. 2003. Specific regulation of the adaptor protein complex AP-3 by the Arf GAP AGAP1. *Dev. Cell.* 5:513–521.

Nie, Z., J. Fei, R.T. Premont, and P.A. Randazzo. 2005. The Arf GAPs AGAP1 and AGAP2 distinguish between the adaptor protein complexes AP-1 and AP-3. *J. Cell Sci.* 118:3555–3566.

Palmer, D.J., J.B. Helms, C.J. Beckers, L. Orci, and J.E. Rothman. 1993. Binding of coatomer to Golgi membranes requires ADP-ribosylation factor. *J. Biol. Chem.* 268:12083–12089.

Pavel, J., C. Harter, and F.T. Wieland. 1998. Reversible dissociation of coatomer: functional characterization of a beta/delta-coat protein subcomplex. *Proc. Natl. Acad. Sci. USA.* 95:2140–2145.

Pepperkok, R., J.A. Whitney, M. Gomez, and T.E. Kreis. 2000. COPI vesicles accumulating in the presence of a GTP restricted arf1 mutant are depleted of anterograde and retrograde cargo. *J. Cell Sci.* 113:135–144.

Poon, P.P., D. Cassel, A. Spang, M. Rotman, E. Pick, R.A. Singer, and G.C. Johnston. 1999. Retrograde transport from the yeast Golgi is mediated by two ARF GAP proteins with overlapping function. *EMBO J.* 18:555–564.

Randazzo, P.A., and D.S. Hirsch. 2004. Arf GAPs: multifunctional proteins that regulate membrane traffic and actin remodelling. *Cell. Signal.* 16:401–413.

Reinhard, C., C. Harter, M. Bremser, B. Brugger, K. Sohn, J.B. Helms, and F. Wieland. 1999. Receptor-induced polymerization of coatomer. *Proc. Natl. Acad. Sci. USA.* 96:1224–1228.

Reinhard, C., M. Schweikert, F.T. Wieland, and W. Nickel. 2003. Functional reconstitution of COPI coat assembly and disassembly using chemically defined components. *Proc. Natl. Acad. Sci. USA.* 100:8253–8257.

Singh, J., Y. Itahana, S. Parrinello, K. Murata, and P.Y. Desprez. 2001. Molecular cloning and characterization of a zinc finger protein involved in Id-1-stimulated mammary epithelial cell growth. *J. Biol. Chem.* 276:11852–11858.

Szafer, E., E. Pick, M. Rotman, S. Zuck, I. Huber, and D. Cassel. 2000. Role of coatomer and phospholipids in GTPase-activating protein-dependent hydrolysis of GTP by ADP-ribosylation factor-1. *J. Biol. Chem.* 275:23615–23619.

Szafer, E., M. Rotman, and D. Cassel. 2001. Regulation of GTP hydrolysis on ADP-ribosylation factor-1 at the Golgi membrane. *J. Biol. Chem.* 276:47834–47839.

Tabas, I., and S. Kornfeld. 1979. Purification and characterization of a rat liver Golgi alpha-mannosidase capable of processing asparagine-linked oligosaccharides. *J. Biol. Chem.* 254:11655–11663.

Tanigawa, G., L. Orci, M. Amherdt, M. Ravazzola, J.B. Helms, and J.E. Rothman. 1993. Hydrolysis of bound GTP by ARF protein triggers uncoating of Golgi-derived COP-coated vesicles. *J. Cell Biol.* 123:1365–1371.

Watson, P.J., G. Frigerio, B.M. Collins, R. Duden, and D.J. Owen. 2004. Gamma-COP appendage domain - structure and function. *Traffic.* 5:79–88.

Wegmann, D., P. Hess, C. Baier, F.T. Wieland, and C. Reinhard. 2004. Novel isotypic gamma/zeta subunits reveal three coatomer complexes in mammals. *Mol. Cell. Biol.* 24:1070–1080.

Yahara, N., K. Sato, and A. Nakano. 2006. The Arf1p GTPase-activating protein Glo3p executes its regulatory function through a conserved repeat motif at its C-terminus. *J. Cell Sci.* 119:2604–2612.

Yang, J.S., S.Y. Lee, M. Gao, S. Bourgoin, P.A. Randazzo, R.T. Premont, and V.W. Hsu. 2002. ARFGAP1 promotes the formation of COPI vesicles, suggesting function as a component of the coat. *J. Cell Biol.* 159:69–78.

Yoshihisa, T., C. Barlowe, and R. Schekman. 1993. Requirement for a GTPase-activating protein in vesicle budding from the endoplasmic reticulum. *Science.* 259:1466–1468.

Zhao, X., A. Claude, J. Chun, D.J. Shields, J.F. Presley, and P. Melancon. 2006. GBF1, a cis-Golgi and VTCs-localized ARF-GEF, is implicated in ER-to-Golgi protein traffic. *J. Cell Sci.* 119:3743–3753.